Journal of The Electrochemical Society, **156** (12) H908-H912 (2009)
0013-4651/2009/156(12)/H908/5/$25.00 © The Electrochemical Society

In Situ Investigation of Slurry Flow Fields during CMP

N. Mueller,[a] C. Rogers,[a] V. P. Manno,[a] R. White,[a,z] and M. Moinpour[b]

[a]*Tufts University, Medford, Massachusetts 02155, USA*
[b]*Intel Corporation, Santa Clara, California 95052, USA*

The objective of this work is to obtain in situ slurry fluid flow data during the chemical mechanical planarization (CMP) process. Slurry flow affects the material removal processes, the creation of defects, and consumable use during CMP, and therefore impacts the cost and quality of polishing. Wafer-scale flow visualization using seeded slurry was accomplished for a variable applied load (0.3–2.5 psi downforce), wafer rotation speed (0 and 33 rpm), slurry injection locations, and various pad types (flat, XY grooved, and AC grooved). In situ pad conditioning was employed in all experiments. The data indicated complex slurry flow fields on the pad surface in the wafer vicinity, which are influenced by slurry injection point, pad grooving, downforce, and wafer/conditioner rotation. Injection location and pad type were shown to have the strongest impact on the variation in the fluid flow fields obtained.
 [DOI: 10.1149/1.3223562]

Manuscript submitted December 29, 2008; revised manuscript received July 31, 2009. Published October 7, 2009.

The semiconductor industry relies heavily on chemical mechanical planarization (CMP) to create planar surfaces on silicon substrates during the integrated circuit (IC) manufacturing process. As the IC feature size continues to shrink, the need to create surfaces with micrometer-level global planarity is of utmost importance.[1-4] CMP is a complex, multimechanism process[1] in which the material removal mechanisms are not well characterized,[5] leading to a high reliance on indirect empirical data.[6] In situ data acquisition during CMP is difficult due to concurrent processes, complex geometries, and the combined opaque nature of the pads, wafers, and slurry during polish. In most cases, CMP data are gathered ex situ or obtained from oversimplified systems that may not fully represent industrially relevant polishing conditions.

Mechanistic models have been developed to explain the phenomena,[3,6-9] but there are only limited empirical data available to test these models. The polishing parameters and their effect on polish quality, which is influenced by fluid transport and polishing components, must be better understood to advance the state of the art in CMP.[1,3,9] The slurry velocity flow fields at the wafer–slurry–pad interface have not yet been fully characterized and a repeatable and reliable method to measure these polishing indicators is lacking.[10] We present data from two flow characterization approaches in this paper: qualitative flow visualization and slurry velocity measurement using particle image velocimetry (PIV).

Experimental

A photograph of the polisher utilized in this work is presented in Fig. 1. The primary component is a modified half-scale Stuers RotoPol-31 CMP industrial polisher that is surrounded by an 80/20 aluminum frame. The polishing system sits atop a 136 kg solid steel isolation table. Optically clear BK-7 glass wafers 75 mm in diameter (3 in.) and 12.5 mm thick (0.5 in.) were rotated and loaded with downforce through the centrally located aluminum shaft driven by a 0.2 hp Dayton motor. A transparent glass wafer was used as a surrogate for a silicon wafer because it has similar polishing characteristics as the semiconductor wafer, but allows optical data acquisition through the wafer to the underwafer region. The wafer was attached to the shaft via a pin connection that allowed the wafer to gimbal.[11] A selection of polyurethane polishing pads 300 mm in diameter (12 in.) was used along with Cabot Microelectronic's Cabo-sil SC-1 oxide polishing slurry with 100 nm fumed silica abrasive particles.[4]

Slurry flow visualization was achieved using tracer particles that were added to the slurry to allow optical tracking of the fluid motion. Pepper particles were used as tracers because they are inexpensive, easy to work with, environmentally benign, and can be imaged under ambient light. To accurately follow the flow, tracer particles need to be small and light enough to travel with the fluid and not perturb the flow. This is usually quantified by the Stokes number of the particle, which should be less than 0.1.[12] However, this is only relevant for neutrally buoyant particles immersed in the flow. The pepper particles used in this study were small enough and had a large enough surface area to be trapped by surface tension at the surface of the flow. We could not, therefore, completely rely on a Stokes number evaluation. However, qualitatively the particles travel with the flow; bubbles and other particulates of various sizes close to the surface of the flow traveled at the same rate as the pepper. Therefore, the pepper behavior was thought to be a good estimate for the fluid behavior.

Video recordings taken at 30 frames/s using a Canon Vixia HG10 high definition video camera were analyzed manually to yield a qualitative description of the slurry flow. Individual flow visualization data acquisition runs were limited to less than 1 min to avoid tracer particle clogging in the pad surface, especially in the grooves. Clogging the pad grooves was avoided because it distorts data interpretation and modifies the flow field. Figure 2 is a sample image in which clogged grooves are apparent.

Several different experimental conditions, including wafer speed, downforce, injection location, and pad type, were examined and compared. The pads used included Freudenberg FX9 flat pads, Freudenberg FX9 XY grooved pads, and Cabot's DC100 ac grooved pads. These pads contained no pattern, a cross-hatched pattern, and a concentric circle pattern, respectively. The specific experimental

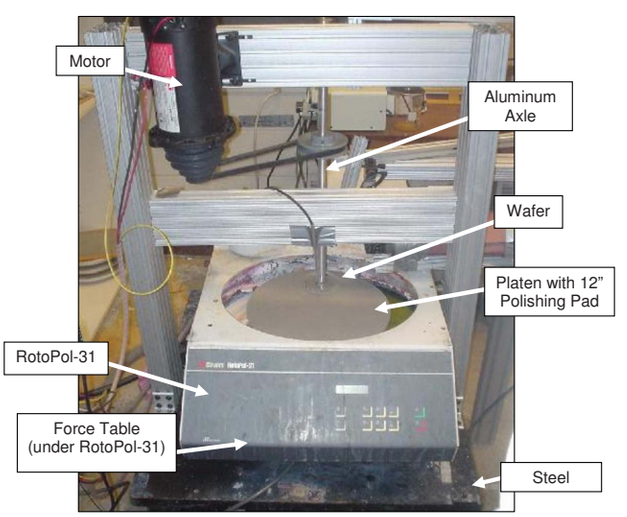

Figure 1. (Color online) The CMP experimental rig used to gather the in situ data. In this photograph the conditioner is not shown so as not to obscure the view, but it is always present during experiments.

[z] E-mail: r.white@tufts.edu

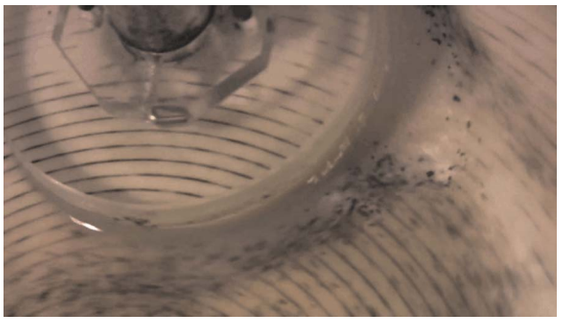

Figure 2. (Color online) A photograph showing the lower half of the wafer and the pepper particle tracers traveling with the slurry flow coming from the bottom right of the image. This image also shows the concentric grooves in the pad becoming clogged with pepper after a long polish.

conditions are seen in Table I. The injection locations are pictured in Fig. 3. Several parameters were held constant throughout polish. The pad rotation was fixed at 30 rpm. During the experiments with wafer rotation, the wafer rotation speed was fixed at 33 rpm, or 10% greater than the platen speed, as commonly used in industrial polishing. This combination of rotational speeds and physical dimensions is equivalent to 2.6 cm/s relative pad–wafer velocity at the wafer center. The slurry was diluted according to the manufacturer-suggested recommendations: three parts deionized water to two parts slurry. The slurry was kept at pH 10 by the addition of potassium hydroxide. The flow rate was fixed at 150 cm^3/min. Before data gathering, each pad was conditioned for 20 min to remove variations in the pad behavior.

PIV was used to quantify the flow characteristics observed. PIV is a well-established flow measurement technique that has the potential to be a useful characterization tool for CMP studies as it yields instantaneous velocity fields in two dimensions without the use of probes or data assembly from repeated smaller measurements.[13] PIV flow data can only be obtained from optically accessible regions of the flow field. A PhotonFocus MV-D1024E complementary metal oxide semiconductor camera was used to gather the images at 19 frames/s at a camera resolution of 400 $\times$ 800 pixels with an exposure time of 100 ms. The camera was capable of acquiring images much faster. However, the increased exposure time necessary to gather enough light through the band-pass filter, centered at 650 $\pm$ 10 nm, severely limited the platen speeds that were measurable. This limitation was due to the available measurement system and is not a fundamental impediment to using PIV at higher rotational speeds.

Any solid particle added to the flow that is large enough for PIV data acquisition would eventually become embedded in the pad and diminish the contrast between particle and background necessary for a PIV quality image. Therefore, a hydrophobic UV fluorescent oil, called OilGlo (Spectronics Corp., Westbury, NY), shown in Fig. 4, was deposited onto the pad in one large droplet, and the CMP polishing system was used to break up the large drop into many smaller PIV size particles. The gathered images were reduced to velocity vectors using digital particle image velocimetry techniques with an error of 0.3 pixel or less. The velocity magnitude calibration methodology was validated using standard processing images and filtering algorithms.[14]

Table I. The experimental conditions.

Wafer speed (rpm)	Downforce (psi)	Injection location	Pad type	Conditioning
0	0.3	Inner	FX9 flat	In situ
33	1	Center	FX9 XY groove	None
	2.5	Outer	DC 100 AC groove	

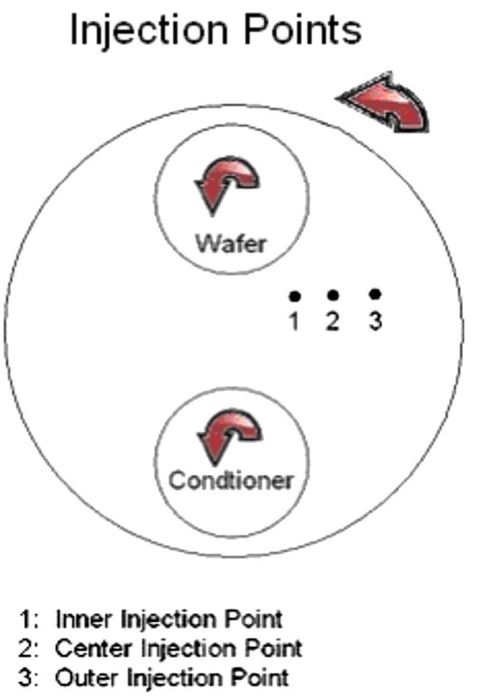

Figure 3. (Color online) A schematic showing the tested injection locations chosen for the flow visualization experiments. The outer injection point was located 5.7 cm from the pad center. The center and inner injection points were located at 8.9 and 14.6 cm from the center of the pad, respectively.

An altered version of the experimental envelope was examined due to the required long exposure times during PIV image acquisition. All measurements were taken on a Freudenberg FX9 polishing pad. The pad was broken in by a conditioner for 20 min before experimentation. The data were gathered at pad speeds ranging from 2 to 5 rpm with the wafer rotating at a speed 10% greater than the platen speed. Slurry was delivered at a rate of 40–50 cm^3/min from the inner injection point.

Results

Flow visualization.— Although wafer speed, downforce, conditioning, injection location, and pad type were varied as part of the experimental envelope examined, only the parametric dependencies of injection location and pad type effects are detailed in this paper.[15] Increased downforce caused the growth of a bow wave created at the upstream wafer edge and changes in the physical extent of the observed flow structures in the vicinity upstream of the wafer. However, major flow characteristics did not change as a result of down-

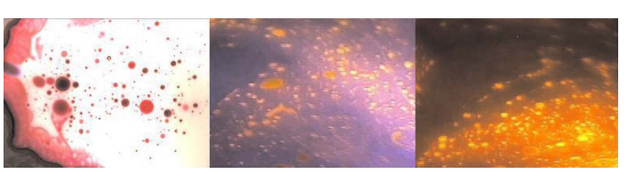

Figure 4. (Color online) Images of the OilGlo UV fluorescent dye used as a PIV tracer. (Left) Under ambient light. (Center) When illuminated with UV light, the oil glows red. (Right) When a filter is added to block out-of-band light, the oil is more easily distinguished.

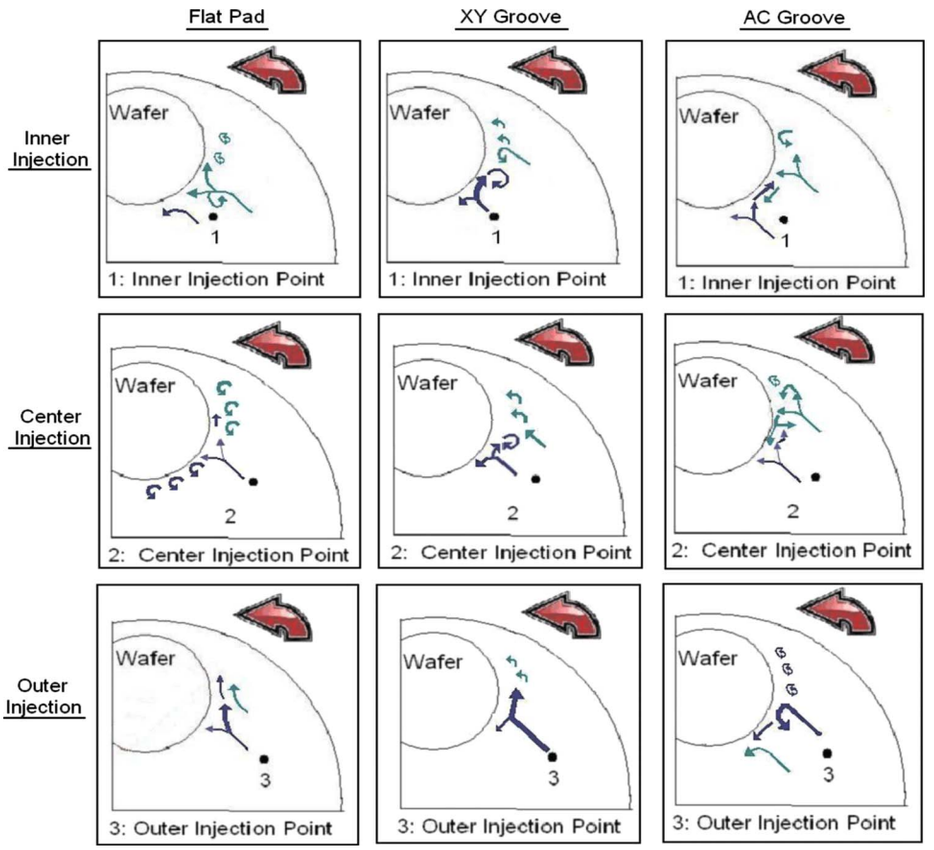

Figure 5. (Color online) The fluid flow fields determined in the flow visualization study are given for three pad types and three injection locations. The conditioner was present, and both pad and wafer were rotating during the experiment. The darker (blue online) vectors represent the path taken by the fresh slurry as it is deposited onto the pad. The lighter (green online) vectors represent the older slurry that has remained on the pad for more than one complete pad rotation.

force. These data corroborate flow visualization data gathered by Copetta et al., who also reported that the downforce had minimal effect.[16]

A summary of the flow fields obtained based on the analysis of the flow visualization video data from the most industrially relevant cases is presented in Fig. 5. The impact of pad type and slurry injection location is easily seen. The darker (blue online) vectors represent the path taken by the fresh slurry as it is deposited onto the pad. The lighter (green online) vectors represent the older slurry that has remained on the pad for more than one pad rotation. This older slurry is potentially chemically depleted as the slurry may have entered the region under the wafer and hence could be depleted in suspended silica particles and carrying wear debris. The latter conditions raise concern about decreased material removal and increased directivity.

The flat pad cases yielded the simplest flow patterns. For the inner injection point, the majority of the slurry interacting with the wafer and performing the polish is older. This is a result of the motion of the fresh slurry toward the middle of the pad after deposition; very little remained at the wafer face. Under these conditions, a small and stable recirculation region forms as this older slurry resides on the pad during rotation. In contrast, the center and outer injection cases have a larger portion of fresh slurry interacting with the wafer face. Though more slurry interacts in the outer injection case, the majority of that fresh slurry is pushed outward and ejected as a result of pad rotation and conditioner presence. The center injection most efficiently enables fresh slurry to be present at the wafer face. As the fresh slurry meets the wafer, the flow smoothly splits with recirculation and passes along the wafer face. Some eddies are formed as a result of the wafer movement, but generally the flow exhibits few regions of high shear.

The XY grooved pad cases yielded more complex flows than those obtained from the flat pad tests. In both the inner and center injection cases, there was increased recirculation of fresh slurry that resulted from its interaction with the older slurry remaining on the pad surface. For the inner injection point, the flow impacts the wafer and, rather than flowing outward as it did with the flat pad, most of the slurry is transported inward along the wafer edge. As that flow comes into contact with the slurry remaining on the pad throughout rotation in the outer half of the wafer diameter, the flows form into two opposing regions of recirculation. The fresh slurry recirculation region is the dominant and stable flow structure in this configuration. The fresh slurry trapped in the recirculation region veers off slightly and enters the smaller region of recirculation before exiting outward. The center injection exhibits a similar pattern. When the fresh slurry reaches the wafer, it splits in the outer half of the wafer diameter and interacts with the old slurry, forming a region of recirculation. If the wafer was larger, a second region of recirculation would likely form as in the inner injection case, but as there is little remaining space along the wafer edge, the majority of the older slurry is forced outward by the region of recirculation. The outer injection tests were similar to the flat pad flow fields.

The AC groove pad test cases produced the most complex flow patterns. The AC groove pattern was reported to exhibit the best slurry transport[8,9] and different flow patterns than flat or *XY* grooved pads. In the cases involving flat and XY grooved pads, the outer injection point seemed to waste the majority of the slurry and flow-starved the inner (i.e., closer to the platen axis of rotation) portion of the wafer diameter. In contrast, for the AC grooved pad, the outer injection enabled slightly more fluid to get to the inner portion of the wafer. However, it also resulted in a large region of slow recirculation upstream of the wafer center. The majority of the fresh slurry appears to get trapped in this region and potentially mixes with older slurry before it interacts with the wafer. There appears to be a region of strong fluid shear in the inner and center injection cases that occurs at the wafer face between regions of fresh and older slurry.

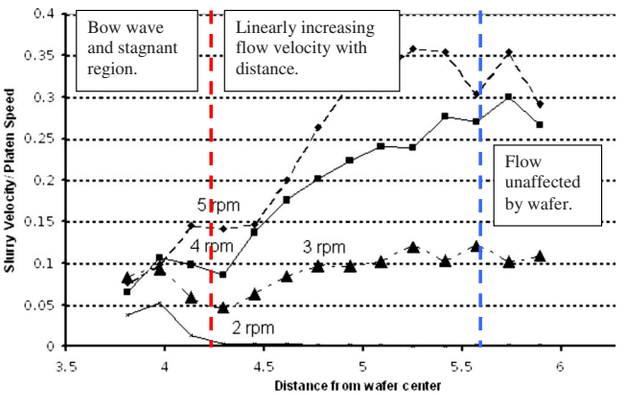

Figure 6. (Color online) Slurry surface speed vs distance from the center of the wafer (in centimeters) is plotted along a line leading from the outer edge of the wafer toward the edge of the pad. The slurry speed is normalized to the platen speed. Three regions are visible in the flow: a bow wave and stagnant region near the wafer, a region of increasing velocity as distance from the wafer increases, and then a region of flow at approximately 30% of the pad velocity that is unaffected by the wafer presence. This result is for an ungrooved FX9 pad with an inner slurry injection point.

However, the inner injection case may be preferable for polishing in CMP as more fresh slurry is delivered to the wafer face.

Taken together, the slurry flow visualization experiments indicated that there are three main regions of flow around the wafer. Directly next to the wafer is a region of fast-moving slurry that is a result of the interaction of the slurry with the moving wafer surface. Following this region, there is a relatively stagnant area that forms the bow wave in front of the wafer. Outside this bow wave, the wafer appears to have minimal effect as the slurry velocity as it increases monotonically with distance from the wafer and pad center.

PIV.— PIV measurements were obtained in an attempt to verify the presence of the three flow regimes seen in the flow visualization tests. The PIV data yielded only comparative values to the flow visualization tests due to limitations in the current PIV system described earlier. In short, the available PIV system, which utilized UV light, required long image exposure times at low light intensity to avoid light flooding of the cameras. The long exposure times and the finite size of the inquiry region allowed only slow rotational speeds to be accessible.

Figure 6 is a synthesis of the most useful PIV data obtained. The vertical axis of Fig. 6 is the slurry surface velocity (as determine by PIV) normalized to the platen speed. The horizontal axis represents distance from the wafer center in centimeters. The result is for an ungrooved FX9 pad with an inner slurry injection point. The data indicate that the slurry velocity is significantly less than the pad velocity. The pad is traveling at approximately 1.6 cm/s in the 2 rpm case, rising linearly to 4 cm/s in the 5 rpm case. At small platen velocities, the ratio between pad and slurry velocity can be as large as an order of magnitude. Keep in mind that the PIV technique, as implemented, only detects surface velocities due to floating oil particles. The slurry surface would necessarily move at slower speeds than the slurry that is in contact with the pad itself. As shown in Fig. 6, a region of flow present near the wafer is relatively stagnant, containing fluid moving at around 10% of the pad speed. After this stagnant region, the fluid speed increased approximately linearly until it reached 30% of the pad speed in the higher rpm cases. The velocity fields located more than 2 cm away from the wafer became increasingly difficult for the PIV system to acquire as the local speeds were too fast for the region of interest. In these locations, the oil particles moved more than half of the window size in a data acquisition time interval and, as such, the PIV accuracy greatly decreased. The fluid speed was at most only 35% of the platen speed in the measurement region.

The data in Fig. 6 confirm the general trend of three distinct flow regimes identified in the flow visualization experiments. Directly next to the wafer is a region of fast-moving fluid that is caused by the motion of the wafer and increased relative speed of the wafer during polishing. This region could not be measured by our PIV setup due to the high velocity. This high velocity region is immediately followed by a region of relatively stagnant flow. This stagnant region might be a result of the buildup of slurry that forms behind the bow wave; the end of that bow wave is indicated by the left vertical line. The slurry velocity appears to linearly increase with distance from the wafer beyond this region. This pattern continues up to the region in which PIV data acquisition is compromised. The 2 rpm case shows a decrease in velocity to zero as the distance from the wafer increases. This is because 2 rpm platen rotation is too slow to impart any real movement onto the slurry. If the region of measurement uncertainty is examined, the slurry begins to increase and appears to reach an asymptotic limit that exhibits much lower than expected velocity measurements resulting from the platen speed in those locations. However, additional testing needs to be conducted with higher image quality to confirm these speculative results. Flow visualization experiments were not performed at these very low rotational speeds because the PIV measurement system has already been validated.[15]

Conclusions

Flow visualization can be an important tool in enhancing the understanding of material removal during CMP. The goal of this research was to demonstrate that flow visualization and PIV measurement could be employed to characterize slurry flow during polishing. Visualization data were taken at industrially relevant rotational conditions while varying pad type, injection location, downforce, wafer speed, and conditioner. The experiments have shown that the flow around the wafer is quite dependent upon process conditions. In particular, slurry injection location and pad type were shown to alter the fluid flow significantly.

Slurry flow is fundamental to understanding CMP process parameter sensitivities. Yet, it has been relatively ignored in the open research literature due to the difficulties in the measurements. The visualization results highlight the complexity of the flow, and the need for further research such as testing over the entire pad region should be conducted to obtain a more complete picture of slurry usage. While the potential for using PIV techniques in the CMP environment was demonstrated in this work, and confirms the qualitative observations from the flow visualization study, more work needs to be done in terms of PIV data acquisition and flow seeding to gather industrially relevant data at higher platen rotation speeds.

Acknowledgments

The authors thank the Semiconductor Research Corporation/Sematech and the National Science Foundation for funding the study. Additionally, special thanks are given to Cabot Microelectronics and Intel Corporation for consumables and advice.

Tufts University assisted in meeting the publication costs of this article.

References

1. L. M. Cook, *J. Non-Cryst. Solids*, **120**, 154 (1990).
2. C. F. Higgs III, S. H. Ng, L. Borucki, I. Yoon, and S. Danyluk, *J. Electrochem. Soc.*, **152**, G193 (2005).
3. S. Runnels and L. Elman, *J. Electrochem. Soc.*, **141**, 1698 (1994).
4. T. F. A. Bibby, J. A. Adams, K. Holland, G. A. Krulik, and P. Parikh, *Thin Solid Films*, **308–309**, 538 (1997).
5. J. Lu, C. Rogers, V. P. Manno, A. Philipossian, S. Anjur, and M. Moinpour, *J. Electrochem. Soc.*, **151**, G241 (2004).
6. W. Tseng and Y. Wang, *J. Electrochem. Soc.*, **144**, L15 (1997).
7. E. Paul, *J. Electrochem. Soc.*, **148**, G305 (2001).
8. S. Runnels, *J. Electrochem. Soc.*, **141**, 1900 (1994).
9. G. P. Mulroney, in *Proceedings of the Materials Research Society Symposium* (2004).

10. C. J. Evans, E. Paul, D. Dornfeld, D. A. Lucca, G. Byrne, M. Tricard, F. Klocke, O. Dambon, and B. A. Mullany, *CIRP Ann.*, **52**, 611 (2003).
11. J. Vlahakis, C. Gray, C. Barns, M. Moinpour, S. Anjur, A. Philipossian, V. Manno, and C. Rogers, in *Proceedings of the 2006 CMP for ULSI Multilevel Interconnection Conference* (2006).
12. C. Tropea, A. Yarin, and J. Foss, *Springer Handbook for Experimental Fluid Mechanics*, pp. 288–289, Springer, New York (2007).
13. J. Waterwheel, Ph.D. Thesis, Delft (1993).
14. M. Raffle, C. E. Willet, and J. Kompenhaus, *Particle Image Velocimetry: A Practical Guide*, Springer, New York (1998).
15. N. Braun, M.S. Thesis, Tufts University, Medford, MA (2008).
16. J. Coppeta, C. Rogers, L. Racz, A. Philipossian, and F. Kaufman, *Journal of CMP for ULSI Multilevel Interconnection*, **1**, 47 (2000).